A Planar Wideband 80–200 GHz Subharmonic Receiver

Brian K. Kormanyos, Paul H. Ostdiek, William L. Bishop, Thomas W. Crowe, *Senior Member, IEEE,* and Gabriel M. Rebeiz, *Senior Member, IEEE*

***Abstract*— A wideband planar subharmonic mixer has been designed for millimeter-wave operation. The receiver consists of a novel back-to-back Schottky-diode pair integrated at the base of a wideband log-periodic antenna and placed on a silicon lens. The wideband planar receiver results in state-of-the art-performance at 90 GHz (and 182 GHz) with a double-sideband conversion loss and noise-temperature of 6.7 dB (and 8.5 dB) and 1080 K (and 1820 K), respectively. These results are about 3 dB higher than the best tuned waveguide subharmonic mixers using planar diodes. The design is well suited for higher frequencies (up to 1 THz) and for the inclusion of biased back-to-back planar diodes to ease the LO power requirements. The planar subharmonic approach results in an inexpensive wideband receiver and the design can be easily extended to receiver arrays.**

I. Introduction

MILLIMETER-WAVE subharmonic mixers use an anti-parallel diode pair to generate a nonlinear conductance waveform at twice the frequency of the applied oscillator (LO) signal [1], [2]. The LO frequency is half the RF frequency, and therefore the isolation between the RF and LO ports is simple. This is commonly done using a suspended-stripline filter, if the LO is waveguide-coupled to the mixer diodes. In the case of a quasi-optical system, the isolation is achieved using a dichroic plate (frequency selective plate). The dichroic plate is simple to construct and will accept a relatively wide range of incidence angles for the RF and LO signals which is important for imaging array design. Another advantage is that for well matched diodes, the mixer generates only odd-order harmonics of the LO signal and there is no DC current flowing through the outside circuit of a subharmonic receiver [3]. This results in a simpler design. The subharmonic design has the advantage of local oscillator noise suppression [4]. The disadvantage of the subharmonic design is increased LO power requirements for unbiased diodes and a potential for higher conversion loss and noise temperature due to unmatched diodes.

Manuscript received September 30, 1992; revised March 11, 1993. This work was supported by the NASA/Center for Space Terahertz Technology at the University of Michigan, and at the University of Virginia by NSF grant ECS-8913169, U.S. Army and Aerojet Electronics.

B. K. Kormanyos and G. M. Rebeiz are with the NASA/Center for Space Terahertz Technology Electrical Engineering and Computer Science Department University of Michigan Ann Arbor, MI 48109-2122.

P. H. Ostdiek is with the Air Force Institute of Technology Department of Engineering Physics Wright-Patterson Air Force Base Dayton, OH 45433.

W. L. Bishop and T. W. Crowe are with the Semiconductor Device Laboratory Department of Electrical Engineering University of Virginia Charlottesville, VA 22903.

IEEE Log Number 9211931.

Currently, all subharmonic mixers are of the waveguide design and are commercially available up to 180 GHz. The mixers typically cover a full-waveguide band and optimal performance is achieved with the use of two waveguide tuners in the RF port and a well matched back-to-back diode pair. This has proven difficult to achieve at millimeter-wave frequencies with the whisker-contacted type, although Carlson and Schneider have built a 205 GHz receiver with 1800 K SSB noise temperature using whisker diodes [5]. Recently, the University of Virginia (UVa) developed a planar back-to-back diode chip suitable for millimeter-wave applications. The diodes are well matched and exhibit a reduced parasitic capacitance due to the surface channel fabrication procedure [6]. Siegel et al. built a 205 GHz waveguide receiver using the UVa back-to-back diodes which resulted in a 1600 K SSB mixer noise temperature [7]. This represents the best result ever for a subharmonic mixer at this frequency. The 205 GHz mixer is complicated to build, requiring two waveguides of different dimensions, 2 E-plane tuners, 2 backshorts and a suspended stripline circuit. This type of mixer is very expensive, especially if built at 600 GHz.

A mixing antenna with quasi-optical RF and LO inputs can result in a much simpler design. A subharmonic mixing antenna has been investigated by Stephen et al. using a bow-tie antenna on a thin dielectric substrate [8]. We have improved the receiver design by combining the planar back-to-back Schottky-diode chip with a wideband log-periodic antenna integrated on a high-resistivity silicon wafer [9]. The log periodic antenna is placed at the back of a silicon lens to eliminate power loss to substrate modes and to render the pattern unidirectional. A polyethylene ($\epsilon_r = 2.3$) quarter-wave matching layer is used at the silicon-air interface to reduce the air-dielectric reflection loss [10]. The LO signal is injected quasi-optically, and the log-periodic antenna catches both the RF and LO signals. An optional matching network can be integrated at the antenna apex for better RF power transfer into the diode pair [11]. The design can be easily implemented with a spiral antenna if a circular polarization is desired. The upper frequency is only limited by the diode design and not the RF coupling (i.e., antenna, and matching networks), and UVa is currently fabricating high quality planar 0.5 μm diodes for 600–800 GHz applications. The planar subharmonic receiver is compatible with the fabrication procedure of the back-to-back diode making this approach fully monolithic. This results in an inexpensive receiver suitable for submillimeter-wave imaging arrays.

0018-9480/93$03.00

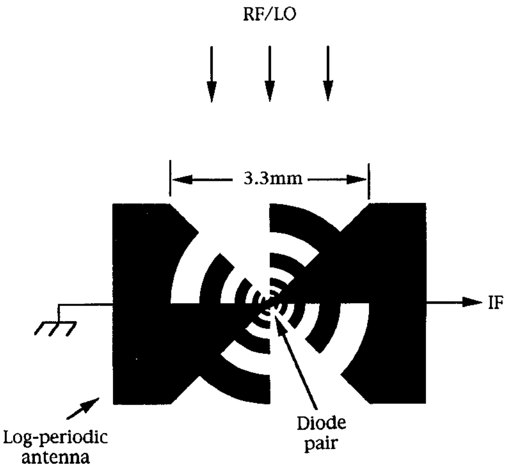

Fig. 1. 26-260 GHz planar log-periodic antenna with $\sigma = 0.707$ and $\tau = 0.5$.

II. Antenna-Lens Design and Measurements

The antenna is a planar self-complementary log-periodic antenna [12] with $\sigma = 0.707$ and $\tau = 0.5$ designed to cover the 26 to 260 GHz band (Fig. 1). The values of σ, τ yield a wideband antenna that maps onto itself every octave. This is advantageous since the LO and RF frequencies are approximately one octave apart. The log-periodic antenna is placed on the back of a silicon lens to eliminate power loss to substrate modes [13]. The dielectric lens also enhances the pattern in the direction of the dielectric and increases the gain. The antenna input impedance is independent of frequency, and is related to the dielectric constant by

$$Z_{\text{ant}} = \frac{189\ \Omega}{\sqrt{0.5(1+\epsilon_r)}} \tag{1}$$

where 189 Ω is the impedance of any self-complementary structure in free-space, and ϵ_r is the relative dielectric constant of silicon. This yields an impedance of 74 Ω for a log-periodic antenna on a silicon lens ($\epsilon_r = 11.7$). As will be seen later, this impedance does not introduce a large mismatch between the antenna and the back-to-back Schottky-diodes. The log-periodic antenna is linearly polarized but shows a considerable cross-polarization component in the E-and H-planes ranging from -5 dB to -14 dB depending on the frequency. The polarization direction of the log-periodic antenna was measured from 35 GHz to 180 GHz and found to vary by ±22.5° with the period given by the teeth geometry (Fig. 2). The polarization measurements fit well the model that the strongest radiation results from the portion of the teeth that is $\lambda_m/4$ long, where λ_m is the mean wavelength calculated using the mean dielectric constant between silicon and air ($\epsilon_m = (1+\epsilon_r)/2$). The radiation mechanism alternates between the left and right teeth and results in the ±22.5° polarization-direction change. The cross-polarization measurements also support this model, being low (-14 dB) when the log-periodic antenna is radiating from the center of a tooth and high (-5 dB) when the log periodic antenna is radiating from both left and right teeth during the transition which occurs just past the $\lambda_m/4$ center frequency for a tooth (Fig. 2). It is also possible to use a self-complementary logarithmic spiral antenna to yield a circularly polarized pattern. In this case, the cross-polarized component is very low (≤ -20 dB) at all frequencies of operation [11]. However, the spiral antenna will exhibit a 3 dB polarization mismatch loss when coupling to a linearly polarized wave.

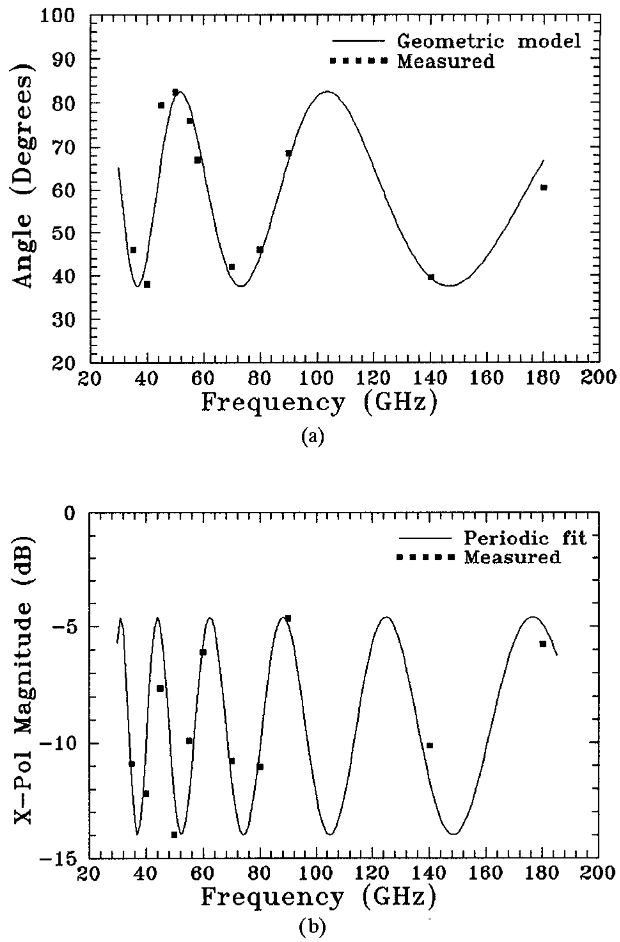

Fig. 2. Measured polarization angle (a) and cross-pol magnitude (b) versus frequency for the log-periodic antenna on the substrate lens.

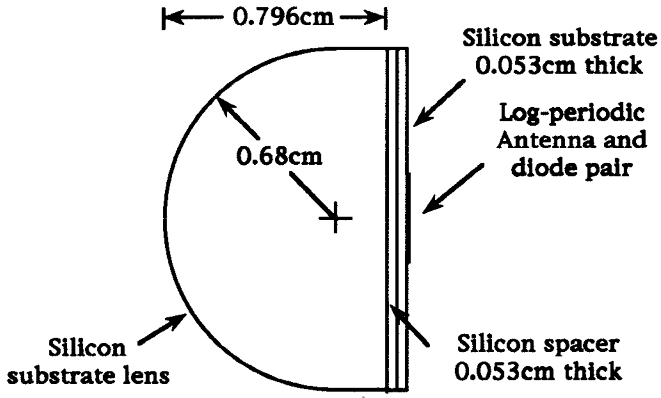

Fig. 3. The extended hemispherical silicon substrate lens.

The log-periodic antenna is placed on an extended hemispherical silicon lens shown in Fig. 3. More precisely, the log-periodic antenna is 2220 μm behind the center of a 0.68 cm-radius hemispherical silicon lens. The spacing wafers with a total thickness of 1070 μm consist of high resistivity silicon substrates (> 2000 Ω−cm). This configuration was chosen

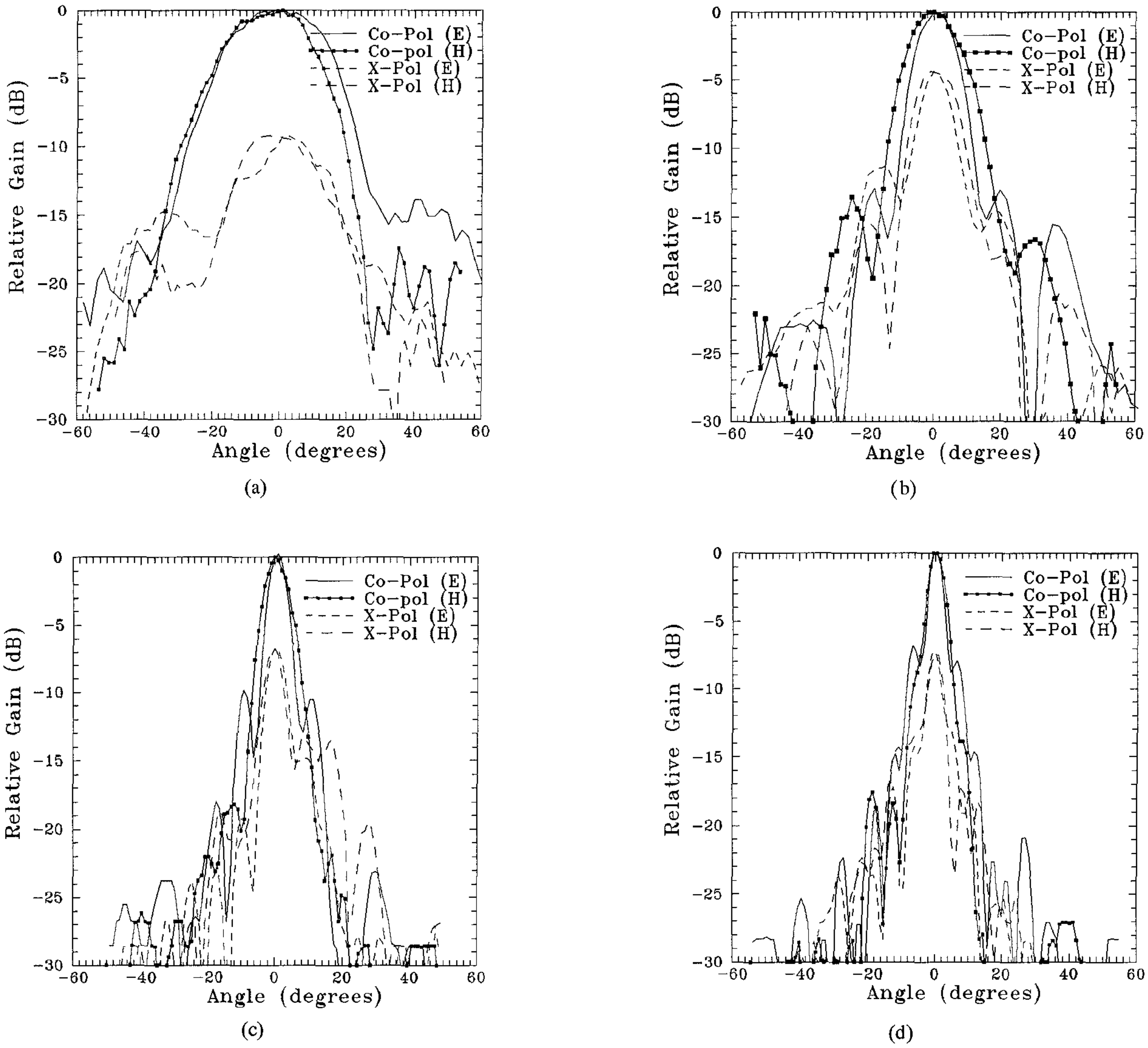

Fig. 4. The measured radiation patterns for the log-periodic antenna on thesubstrate lens at 40 GHz (a), 90 GHz (b), 180 GHz (c), and 250 GHz (d).

after a ray-optics based calculation by Filipovic et al. on the gaussian-coupling and directivity properties of hyperhemispherical and extended hyperhemispherical lenses (see [14]). The calculations were performed for double-slot and double-dipole antennas with symmetric patterns and it was found that a position between 2200 and 2400 μm yields good high gain patterns and good gaussian coupling efficiencies (85%) in the frequency range from 100 to 500 GHz. It is important to note that the hyperhemispherical position of 2000 μm yields an even higher theoretical coupling efficiency (90%) but at the expense of lower gain and therefore lower f-number imaging systems. The position of 2220 μm is seen as a compromise between high gain patterns needed for large f-number quasi-optical systems and a small reduction in the gaussian-coupling efficiency. The log-periodic antenna was, of course, not analyzed in [14]. However, a 2220 μm position is chosen for the subharmonic mixer and, as will be seen later, resulted in good patterns and gaussian-coupling efficiencies.

Fig. 4 shows the measured E and H-plane patterns of the log-periodic antenna at 40 GHz, 90 GHz, 180 GHz and 250 GHz placed at the 2220 μm position. The 45°-plane patterns are very similar to the E-plane patterns and are not shown. The cross-polarization pattern is very similar to the co-polarized pattern but with a -5 dB to -14 dB peak depending on the frequency. Only a small amount of power radiates from the back side of the substrate lens. The back side patterns (not shown) are wider and at least -20 dB from the front side patterns. The matching gaussian beams at 90 GHz and 180 GHz are discussed in the mixer measurement section (Section IV). If the log-periodic is placed at a position of 2750 μm behind the hemispherical center, an elliptical lens is closely approximated. Patterns with lower sidelobes are achieved at 180 GHz and 250 GHz in this position but at an expense of lower gaussian coupling efficiency (see [14]). It is important to note that the log-periodic antenna pattern inside the dielectric substrate lens is frequency independent but the lens acts as a circular aperture of approximately

TABLE I
MEASURED PARAMETERS FOR BOTH JUNCTIONS ON THE BACK-TO-BACK DIODE CHIP.

Diode SR2T1	Anode dia. (μm)	C_{jo} (fF)	Is (Amps)	Ideality factor	Rs (Ω)	ϕ_{bi} (Volts)
Junction 1	1.3	4	8.9×10^{-17}	1.20	10.8	0.84
Junction 2	1.3	4	1.9×10^{-17}	1.14	11.4	0.88

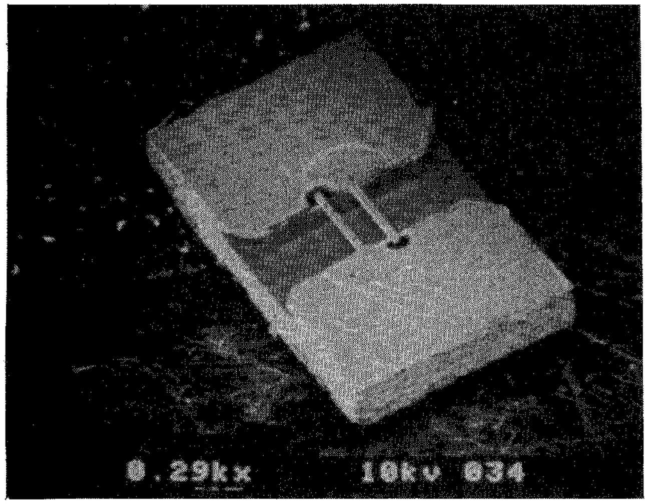

Fig. 5. SEM picture of the surface channel back-to-back diode chip before GaAs substrate thinning.

constant dimension resulting in narrowing far field patterns as frequency increases.

III. DIODE CHARACTERISTICS AND RF MEASUREMENTS

The GaAs anti-parallel Schottky-diode chip, shown in Fig. 5, is an SR2T1 type developed and fabricated at the University of Virginia. The chip is 250 μm long and 125 μm wide. The anode and cathode contact pads are 125 μm $\times$ 100 μm. The finger length is 50 μm with a thickness of 2 μm and width of 3 μm. A surface channel technology has been used to eliminate the conducting path between the anode and cathode pads [15] and to reduce the parasitic capacitance between the anode and cathode. The parasitic capacitance is further minimized by thinning the GaAs wafer to 7 μm and placing it on a quartz substrate for mechanical rigidity considerations. Details of the fabrication procedure and the substrate thinning technique are presented in [16]. The diode chip is then epoxied at the antenna apex using a low-temperature process. The quartz substrate can be removed after the chip is bonded in place by simply dissolving the adhesive [16] between the GaAs chip and the quartz substrate. However, in this work, the quartz substrate was kept attached to the diode. The diodes consist of a 900Å n^- layer doped at $2 \times 10^{17}/\mathrm{cm}^3$ backed by a 5 μm n^+ layer doped at $3 \times 10^{18}/\mathrm{cm}^3$.

The diodes have an average anode diameter of 1.3 μm, a measured DC series resistance of 11 Ω and a zero-bias capacitance of 4fF. The diodes are very similar with an ideality factor n = 1.2, a barrier height of 0.85 V and a turn on voltage of 0.7 V at 1 μA (see Table I). The total parasitic capacitance for the quartz- supported diode is estimated at 3-4fF, thereby yielding a figure-of-merit cutoff frequency of approximately 2 THz.

Video detection measurements were done at 90 GHz and 180 GHz by shining a plane wave with a known power density on the log-periodic/substrate lens antenna and measuring the output detected voltage in a 106 KΩ load using a lock-in amplifier. The RF plane-wave is calibrated to ±5% using an Anritsu power meter at 90 GHz and a large-area bolometer at 180 GHz [17]. The video responsivity is defined here as the ratio of the detected low-frequency voltage across a 106 KΩ load divided by the RF power available at the terminals of the log-periodic antenna. This definition eliminates the effect of the planar antenna and results in an RF source with a constant impedance of 74 Ω at 90 GHz and 180 GHz. The available power, P_{av}, at the antenna terminals is given by

$$P_{av} = S A_e \Gamma_l \alpha_s \tag{2}$$

where S is the incident power density, A_e is the effective aperture of the log-periodic/silicon lens antenna calculated from the measured directivity, D_a, using the formula $A_e = (\lambda^2/4\pi) D_a$. The directivity is in turn calculated using full-two dimensional measurements of the co-polarized and cross-polarized patterns with a signal-to-noise ratio of better than 40 dB and standard textbook formulas [18]. Γ_l is the loss at the silicon-air interface calculated using simple transmission-line analysis to be 1.5 dB and α_s is the dielectric loss in the 1000 Ω−cm silicon lens estimated to be 0.5 dB [19].

The measured and theoretical video responsivity at 90 and 180 GHz are shown in Fig. 6. The diode parameters used are a series resistance of 11 Ω, a zero-bias junction capacitance of 4 fF, an ideality factor of 1.2 and a barrier height of 0.85 V. The model has one free parameter, the parasitic capacitance, chosen to be 3 fF. The peak video responsivity is 2600 V/W at 90 GHz and 1100 V/W at 180 GHz and is competitive with whisker diodes at these frequencies. The model fits well the measurements at 90 GHz and 180 GHz without changing any of the diode parameters between the two frequencies. Since the absolute power density is known to ±5% and the estimated error in the antenna directivity is ±5%, the capacitance estimate from video responsivity measurements is accurate to about 2 fF. The results do confirm the DC measured values of the total diode capacitance and that the thinning procedure results in a lower parasitic capacitance.

IV. MIXER MODELING AND MEASUREMENTS

A. Nonlinear Analysis

A nonlinear program was written at the University of Michigan for the analysis of subharmonic mixers. The program

TABLE II
RESULTS FROM NON-LINEAR ANALYSIS FOR THE SUBHARMONIC MIXER (LO AND RF EMBEDDING IMPEDANCES ARE 74 Ω, IF IMPEDANCE IS 110 Ω).

F_{Lo} (GHz)	F_{RF} (GHz)	Lo Power (mW)	RF Impedance (Ω)	Lo Impedance (Ω)	If Impedance (Ω)	Conversion Loss (SSB) (dB)
45	90	5.0	42-j71	72-j284	154	8.0
-	-	6.6	44-j48	91-j226	98	7.6
-	-	8.0	44-j35	93-j193	75	8.3
91	182	6.0	17-j40	20-j142	140	10.3
-	-	7.6	18-j37	24-j133	108	9.6
-	-	9.0	21-j34	27-j123	84	9.8

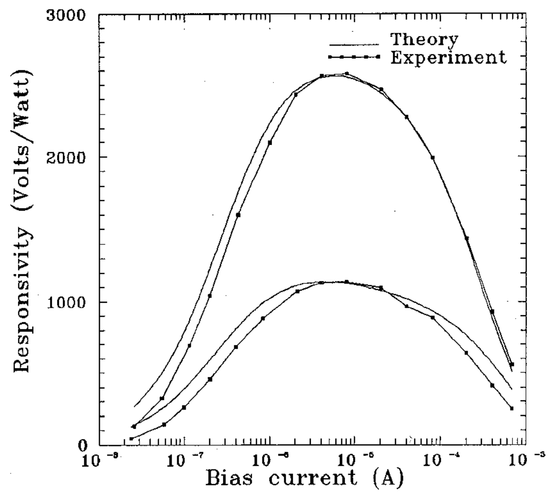

Fig. 6. Measured video responsivity versus bias current for the diodes at 90 GHz (2600 V/W peak) and 180 GHz (1100 V/W peak).

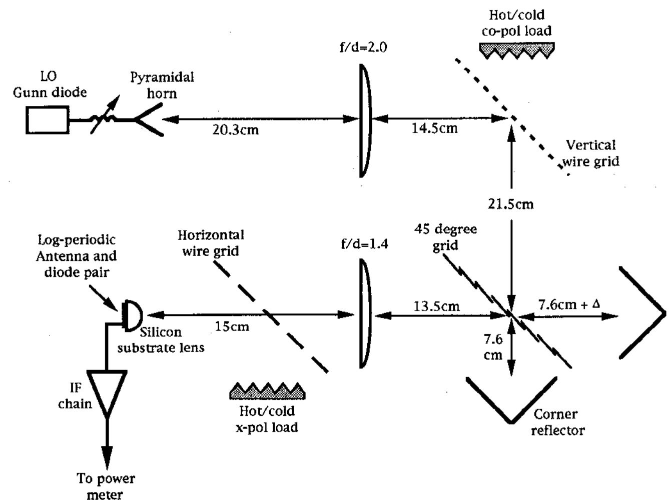

Fig. 7. Quasi-optical setup for measuring DSB conversion loss and noise temperature.

is based on the reflection algorithm developed by Kerr *et al.* [20] and takes into account the asymmetrical I-V curve of the back-to-back diodes. This is done by splitting the antiparallel diodes into two equivalent single diodes with LO terminating impedances set to zero for even harmonics and DC [3]. The higher order terminating impedances at $3f_{Lo}, 5f_{lo}$ and $7f_{Lo}$ are taken to be the wideband antenna impedance of 74 Ω in parallel with the parasitic capacitance of the diode. All impedances at higher harmonics are assumed to be short-circuited. The analysis was done for the conversion loss only and the results for a 90 GHz RF and a 182 GHz RF are summarized in Table II. The analysis indicates that a single-sideband conversion loss of 7.6 dB and 9.6 dB are attainable at 90 GHz and 182 GHz, respectively, without an RF matching network. The available LO power at the antenna apex is 6.6 mW at 45 GHz and 7.6 mW at 91 GHz. The corresponding RF, LO and IF impedances are shown in Table II and result in an LO mismatch of 1.6 dB at 45 GHz and 2.8 dB at 91 GHz. It is possible to improve the conversion loss by 1 dB at 90 GHz and 2.7 dB at 182 GHz with an RF matching network at the apex of the antenna. The penalty is a reduction in bandwidth.

B. Quasi-Optical System and Receiver Setup

The quasi-optical measurement setup is shown in Fig. 7. A dichroic plate was not available for this experiment and a Martin–Pupplett diplexer was used to inject the local oscillator to the subharmonic mixer. The Martin–Pupplett uses polarization grids and its response is therefore independent of frequency. It can be easily configured to pass the LO signals from the LO port and the upper and lower sideband RF signals at approximately twice the LO frequency from the RF port (Fig. 8). However, the Martin–Pupplett also passes the upper and lower sidebands of the LO signal from the RF port. Therefore, one must be careful that fundamental mixing is not occurring at the diode terminals. This is achieved by using well balanced back-to-back diodes that inherently eliminate the fundamental mixing mechanism. The back-to-back diode DC current in the outside loop was around 80 μA for an estimated available 45 GHz LO power of 9 mW at the diode terminals. This is about 30 times smaller than what is expected from a single diode at comparable LO power and is an indication that the back-to-back diodes are well balanced and suppressing fundamental mixing.

The quasi-optical measurement setup provides a two lens system for coupling the LO signal from the Gunn source to the mixer. The RF signal is coupled to the hot-cold load through only one of the lenses. The lens system was designed by determining the beamwaist of the antenna from the measured patterns. LO coupling through the two lens system is optimized at 91 GHz. LO coupling at 45 GHz is less of a concern since there is an excess of available power from the source. RF signals at both 90 GHz and 182 GHz are well coupled to the absorber through the f-number 1.4 objective lens. The diffraction loss in the Martin–Pupplet diplexer is estimated

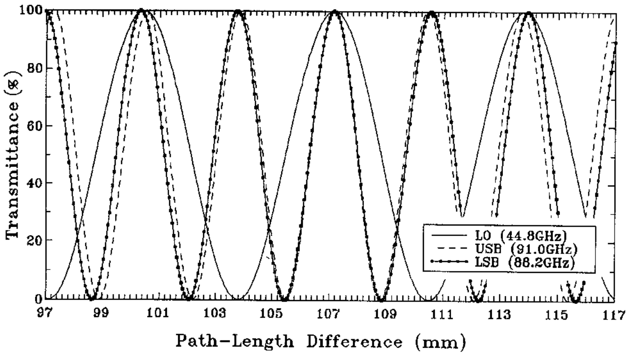

Fig. 8. Theoretical power transfer function for the Martin–Pupplet polarization rotating diplexer versus path length difference (107.14 mm optimum).

to be 0.2 dB. The lenses are 10 cm diameter Rexolite with estimated total reflection and dielectric losses of 0.6 dB at 90 GHz and 0.8 dB at 182 GHz. These are taken out of the measurements for the noise figure and conversion loss. The pertinent dimensions in the quasi-optical LO injection system are shown in Fig. 7.

A horizontal polarization grid is placed at 45° in front of the log-periodic/silicon lens antenna to reflect the cross-polarized component into a hot-cold load. In this configuration, both the copolarized and cross-polarized components contribute to the RF signal. This measurement method simulates well a dichroic plate which can be designed to pass both RF polarizations. The hot-cold load is an Eccosorb AN-72 and the cold temperature is estimated to be 85 K at millimeter-wave frequencies [21]. A polyethylene matching cap layer was used at 90 GHz RF and 182 GHz RF and improved the noise temperature and conversion loss by 0.6 dB. This was lower than the expected value of 1.2 dB due to the difficulties encountered in building a thin spherical plastic lens cover. The available LO power at the diode terminals is estimated by measuring the total radiated power at 45 GHz and 91 GHz and then normalizing out the dielectric reflection and absorption loss in the two lens system, the dielectric reflection and absorption loss in the silicon lens and the gaussian coupling efficiencies of the pyramidal LO horn (estimated to be 60%) and the log-periodic/silicon lens. The IF chain consists of a 10 dB coupler, a bias-T to measure the outside DC current, a circulator, a low-noise amplifier chain, a 100 MHz band-pass filter centered at 1.4 GHz and a calibrated IF power meter. The 10 dB coupler is used to measure the IF reflection coefficient and is removed for standard receiver measurements. The IF chain has a gain of 98.5 dB and a 96 K noise temperature without the 10 dB coupler.

C. 90 GHz and 182 GHz Measurements

The measured double-sideband conversion loss and noise temperature at 90 GHz and 182 GHz versus available LO power at the diode terminals are shown in Fig. 9. The conversion loss and noise temperature are referenced to a hypothetical plane in front of the log-periodic/silicon lens and include the antenna gaussian coupling efficiency (estimated to be around −0.7 dB), the residual reflection loss (−0.9 dB) and absorption loss (−0.5 dB) in the silicon lens, the diode

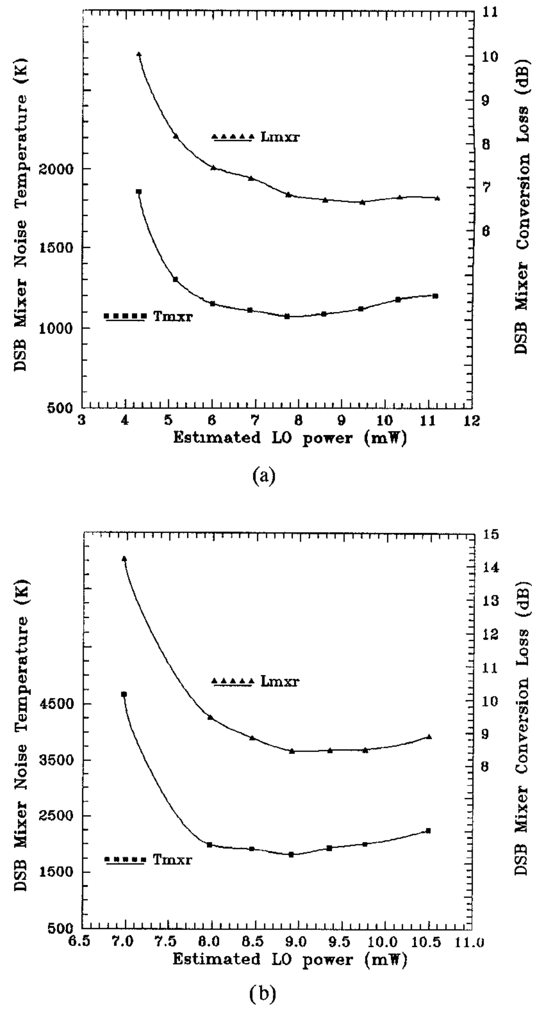

Fig. 9. Measured conversion loss and noise temperature at 90 GHz (a) and 182 GHz (b) versus estimated LO power available at the antenna terminals.

intrinsic conversion loss, the mismatch between the log-periodic antenna and the back-to-back diodes and the IF mismatch at 1.4 GHz. A minimum DSB conversion loss of 6.7 dB at 90 GHz and 8.5 dB at 182 GHz is attained at an available LO power of about 9 mW (Fig. 9). Agreement with the non-linear analysis is good when the antenna and silicon lens losses are taken into account. At 182 GHz the minimum DSB noise temperature of 1820 K is attained simultaneously with the minimum conversion loss. At 90 GHz a minimum DSB noise temperature of 1070 K is measured experimentally at a lower LO power of 8 mW. At both frequencies the IF impedance is experimentally determined to be about 110 Ω using an IF power reflection measurement. A microstrip matching network is used to reduce the IF reflection coefficient to less than 0.1 dB for minimum noise-temperature measurements. The noise temperature and conversion loss were about 2 dB higher if the cross-polarization component was not cooled, but terminated in a room temperature absorber. This shows that a significant fraction of the power is in the cross-polarized component and that it should not be ignored when using a log-periodic antenna on a dielectric lens for receiver measurements.

V. Conclusion

A wideband quasi-optical subharmonic receiver has been built for millimeter-wave applications. The receiver is based on a wideband log-periodic antenna placed on a silicon substrate lens and a back-to-back diode. The polarization properties of the planar log-periodic antenna on a silicon substrate lens have been investigated from 35 GHz to 180 GHz. It was found that the antenna exhibits a ±22.5° periodic polarization change given by the antenna geometry and a periodic change in the cross-pol magnitude (between −5 dB and −14 dB). The receiver exhibits excellent room temperature performance being only 3 dB higher than the best waveguide mixers at 182 GHz. This is due to the use of a planar back-to-back diode with low parasitic capacitance and the characterization of the log-periodic antenna and its optimal placement on a dielectric lens. The receiver is monolithic and can easily operate from 80 GHz to 260 GHz with the use of appropriate dichroic plates. Furthermore, the receiver performance may be improved by 2–3 dB with the inclusion of an RF matching network at the apex of the antenna.

References

[1] M. Cohn, J. E. Degenford, and B. A. Newman, "Harmonic mixing with an antiparallel diode pair," *IEEE Trans. Microwave Theory Tech.,* vol. MTT-23, pp. 667–673, Aug. 1975.

[2] M. V. Schneider and W. W. Snell, "Harmonically pumped stripline downconverter," *IEEE Trans. Microwave Theory Tech.,* vol. MTT-23, pp. 271–275, Mar. 1975.

[3] A. R. Kerr, "Noise and loss in balanced and subharmonically pumped mixers: Part I-theory", and Part 2 experiment," *IEEE Trans. Microwave Theory Tech.,* vol. MTT-27, no. 12, pp. 938–950, Dec. 1978.

[4] P. S. Henry, B. S. Glance and M. V. Schneider, "Local oscillator noise cancellation in the subharmonically pumped down converter," *IEEE Trans. Microwave Theory Tech.,* vol. MTT-24, pp. 254–7, May 1976.

[5] E. R. Carlson and M. V. Schneider, "Subharmonically pumped millimeter-wave receivers," *Dig. 4th Int. Conf. on Infrared and Millimeter Waves,* Dec. 10–15 1979, pp. 82–83.

[6] P. H. Ostdiek, T. W. Crowe and I. Galin, "Integration of an anti-parellel pair of Schottky barrier diodes in millimeter-wave mixers," *15'th Int. Conf. Infrared and Millimeter Waves,* Orlando, FL, Dec. 1990.

[7] P. H. Siegel *et. al.* "A 200 GHz planar diode subharmonically pumped waveguide mixer with state-of-the-art performance," *Dig. IEEE MTT-S Int. Microwave Symposium,* vol. 2, pp. 595–598, Albuquerque, New Mexico June 1–5 1992.

[8] K. D. Stephan and T. Itoh, "A planar quasi-optical sunharmonically pumped mixer characterized by isotropic conversion loss," *IEEE Trans. Microwave Theory Tech.,* vol. MTT-32, no. 1, Jan. 1984.

[9] B. K. Kormanyos *et. al.,* "A planar wideband millimeter-wave subharmonic receiver," *IEEE MTT-S Int. Symp.,* Boston, MA., June 1991, pp. 213–216.

[10] C. E. Zah, and D. B. Rutledge, "A polystyrene cap for matching a silicon lens at millimeter wavelengths," *J. Infrared and Millimeter Waves,* vol. 6, pp. 909–918, Sept. 1985.

[11] T, H. Buttgenbach, H. G. LeDuc, P. D. Maker, and T. G. Philips," A fixed tuned broadband matching structure for submillimeter SIS receivers," *IEEE Trans. Applied Superconductivity,* Sept. 1992.

[12] R. H. DuHamel and D. E. Isbell, "Broadband logarithmically periodic antenna structures," Tech. Rep. no. 19, Antenna Lab, U. of Illinois, May 1957; also *IRE National Convention Rec.,* Part-1, 1957.

[13] D. B. Rutledge, D. P. Neikirk and D. P. Kasilingam, "Integrated circuit antennas," in *Infrared and Millimeter Waves,* vol. 10, pp. 1–90, K. J. Button, Ed., New York: Academic Press, 1983.

[14] D. F. Filipovic, S. S. Gearhart and G. M. Rebeiz, "Double slot antennas on extended hemispherical and elliptical lenses," *IEEE Trans. Microwave Theory Tech.,* this issue.

[15] W. L. Bishop *et. al.* "A novel whiskerless diode for millimeter- wave and submillimeter-wave applications," *IEEE MTT-S Int. Symp.,* Las Vegas, NV, June 1987, pp. 607–610.

[16] ——., "A micron thickness planar Schottky diode chip for terahertz applications with theoretical minimum parasitic capacitance," *IEEE MTT-S Int. Symp.,* Dallas, TX, May 1990, pp. 1305–1308.

[17] C. C. Ling, and G. M. Rebeiz, "A wide band monolithic quasi-optical power meter for millimeter- and submillimeter-wave applications," *IEEE Trans. Microwave Theory Tech.,* vol. 39, no. 8, pp. 1257–1261, Aug. 1991.

[18] R. S. Elliott, *Antenna Theory and Design.* Englewood Cliffs, NJ: Prentice-Hall, 1981.

[19] M. V. Afsar and K. J. Button, "Millimeter-wave dielectric properties of materials," *Infrared and Millimeter Waves,* vol. 12, Ch. 1, pp. 1–42, 1984.

[20] P. H. Siegel and A. R. Kerr, "A user oriented computer program for the analysis of microwave mixers, and a study of the effects of the series inductance and diode capacitance on the performance of some simple mixers," NASA Goddard Space Flight Ctr., Greenbelt, MD, NASA Tech. Memo. No. 80324, July 1979.

[21] W. Y. Ali-Ahmed, G. M. Rebeiz, W. L. Bishop, and T. W. Crowe, "An 86-106 GHz quasi-integrated low noise Schottky receiver, *IEEE Trans. Microwave Theory Tech.* vol. 41, no. 4, pp. 558–564, Apr. 1993.

[22] J. D. Dyson, "The equiangular spiral antenna," *IEEE Trans. Antennas Propagat.,* pp. 181–187, Apr. 1959.

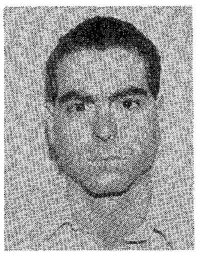

Brian K. Kormanyos was born in September, 1966. He received a B.S. degree in electrical engineering from the University of Washington in 1989. In 1991 he received a M.S. degree in electrical engineering from the University of Michigan, Ann Arbor where he is currently enrolled in a Ph.D. program. His research is in millimeter-wave receivers and sources.

Paul H. Ostiek received a B.S. degree in physics at the U.S. Air Force Academy in 1979. In 1984 he received his M.S. degree in Engineering Physics from the U.S. Air Force Institute of Technology as a distinguished graduate. He earned his Ph.D. in electrical engineering from the University of Virginia in 1991. Paul Ostdiek is a Major in the U.S. Air Force, currently serving as an assistant professor at the U.S. Air Force Institute of Technology. His current research interests include materials characterization (photo/cathodo-luminescence), device fabrication, and radiation effects on electronics.

William L. Bishop received the B.S. degree in engineering science from the University of Virginia, Charlottesville, in 1969.

He is presently a Research Scientist in the Semiconductor Device Laboratory at the University of Virginia. His primary interest is the design and fabrication of planar Schottky diodes for high frequency applications.

Thomas W. Crowe (S'84–M'87–SM'91) received the B.S. degree (physics) from Montclair State College, Montclair, NJ, in 1980. Since that time he has been at the University of Virginia. He received the M.S.E.E. degree from the University of Virginia in 1982, and the Ph.D. degree in electrical engineering in January 1986. He became a Research Assistant Professor of Electrical Engineering in March of 1986 and a Research Associate Professor in July of 1991. Since January of 1989 he has been the Director of the Semiconductor Device Laboratory.

His main areas of interest are the development of high frequency semiconductor devices and the optimization of solid-state devices for use in low noise submillimeter wavelength receivers. His present research is focused on the investigation of novel device structures for high frequency applications, development of solid-state power sources for THz frequencies and the use of planar device technologies to allow the routine implementation of heterodyne receivers on space platforms. He also has interests in semiconductor noise theory and the numerical modeling of semiconductor devices.

Dr. Crowe is a member of Sigma Xi, Eta Kappa Nu, and URSI.

Gabriel M. Rebeiz (S'86–M'88–SM'92) was born in December 1964 in Beirut, Lebanon. He graduated in 1982 from the American University in Beirut with a B.E. (Honors) in electrical engineering. In September 1982, he joined the California Institute of Technology and earned the Ph.D. in electrical engineering in June 1988. He joined the faculty of the University of Michigan in September 1988 where he is now an Associate Professor in the Electrical Engineering and Computer Science Department.

Dr. Rebeiz has been awarded a NASA-Certificate of Recognition Award for his contribution to the millimeter-wave space program (March 1990) and the Best Paper Award at the 1990 International Conference on Antennas, Nice, France. He received an NSF Presidential Young Investigator Award in 1991, and was elected member of URSI-D in January 1992. His research interests lie in planar millimeter-wave antennas, receivers and transmitters, and fabrication and measurements of novel transmission-lines and devices.

In August 1993, he received the URSI Koga Gold Medal Award for outstanding research under 35.